



AN EXPERIMENTAL STUDY OF BUCKLING RESTRAINED BRACE WITH INSPECTION WINDOWS

C. S. Tsai⁽¹⁾, Yi Liu⁽²⁾, B. Q. Liu⁽³⁾

⁽¹⁾ Distinguished Professor, Department of Civil Engineering, Feng Chia University, Chinese Taipei, cstsai@mail.fcu.edu.tw

⁽²⁾ Master Student, School of Civil Engineering, Chang'an University, Xian, China, LiuYi90123@163.com

⁽³⁾ Professor, School of Civil Engineering, Chang'an University, Xian, China Email: bqliu@chd.edu.cn

Abstract

The buckling restrained brace (BRB) has been implemented worldwide in structures to prevent them from earthquake damage. However, the steel core of the traditional BRB is enclosed by the buckling-restraining unit, it is therefore impossible to observe the condition of the steel core during manufacturing and after earthquakes. Presented in this paper is an experimental research on a buckling restrained brace with inspection windows that allow direct observation of the condition of the BRB internal components. Experimental study on deciding the sizes and locations of the inspection windows without influencing the functionality of the BRB were conducted to search for a feasible BRB that is economical and convenient for manufacturing and installation as well as meets testing protocols. Test results of the scaled BRBs under cyclic loadings show that the mechanical behavior of the scaled BRB with inspection windows opened on the buckling-restraining unit is stable and that fracture always occurs at the energy dissipation segments after low cycle fatigue tests. The condition of the steel core can be clearly observed through the inspection windows during the tests. The test results also indicate that the selected inspection windows on the scaled BRB have little influence on the strength of the device. It is concluded that an appropriately designed BRB device with inspection windows can be considered as a stable energy dissipation device.

Keywords: buckling restrained brace; energy absorption system; passive control; earthquake engineering

1. Introduction

As shown in Fig. 1, the concept of using a tube as a lateral support to prevent a steel rod subjected to an axial load from buckling was first, to the best of authors' knowledge, proposed by Hollander in 1966 [1]. Since the 1970s, the buckling-restrained brace (BRB) has been adopted worldwide to avoid buckling for the traditional brace under repeated loadings during an earthquake. Wakabayashi et al. [2] proposed a brace system made by one steel core plate enclosed by two precast concrete wall panels to prevent the brace from buckling under loadings in 1973. In 1976, Kimura et al. [3] presented another type of BRB in virtue of encasing the steel core in a mortar-filled steel tube. Mochizuki et al. [4] performed tests on the braces with a layer of shock-absorbing material to avoid the bonding between the steel core and the concrete, and to allow transverse expansion of the steel core in compression in 1979. Basically, a BRB is usually composed of three major components: the steel core, the buckling-restraining unit, and the de-bonding material. Wada et al. [5] in 1992 suggested that the BRB would be designed as a damper to dissipate seismic energy. Black et al. [6] in 2002 and Merritt et al. [7, 8] in 2003 carried out the standard and low-cycle fatigue tests of BRBs to investigate their characteristics. However, special attention needs be paid to several shortcomings of the traditional BRBs that use mortar encased in a steel tube to prevent the steel core from buckling [1-10]. These shortcomings include: (1) the complexity of the interfaces between adopted materials to cause uncertain fabricating quality, (2) time consuming during the manufacturing processes, and (3) difficulties in monitoring the manufacturing quality and detecting the damage levels after an earthquake.

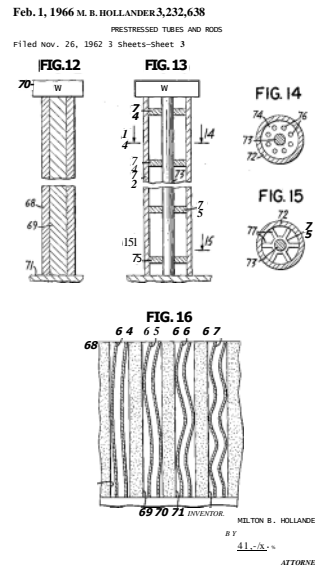


Fig. 1 – Hollander's original patent (1966, US Patent No. 3,232,638)

As a feasible solution to the abovementioned problems, all-steel buckling-restrained braces (all-steel BRBs) that have no demands on un-bonding materials and mortar, or complicated manufacturing interfaces among different materials, have been proposed to overcome the disadvantages of the traditional BRBs [11-18]. The all-steel BRB consists of the steel core that is typically separated from the steel buckling-restrained unit by a small gap in the necessary direction. Furthermore, the all-steel BRBs can be demounted to enable inspection and monitoring, if bolt connections are used between the steel core and the buckling-restrained unit. In 2008 and 2009, a new type of all-steel BRB called the multi-curve BRB (MC-BRB) was proposed by Tsai et al [15, 16]. It consisted of a single steel core plate with an enlarged segment in the middle of the steel core to form a multi-curved shape, and a buckling-restrained unit that included constraining elements and lateral support elements. Zhao et al. [19] in 2011 carried out a series of studies on the MC-BRB and concluded that the MC-BRB possesses more stable mechanical characteristics than the traditional BRBs and requires no de-bonding material. To examine the mechanical behavior of the large-scale all-steel MC-BRB, the component tests of an all-steel MC-BRB with double steel core plates designed to sustain an axial force of 14000 *kN* were performed in 2012, Taiwan [20]. The results demonstrated that this type of MC-BRB possesses stable mechanical behavior under cyclic loadings, and provides excellent inelastic deformation capacity [20]. However, the steel cores of the abovementioned BRBs are fully enclosed by the buckling-restraining unit, it is therefore impossible to inspect the condition of the inside steel cores after manufacturing and earthquakes without dismantling the devices. In addition, it will be difficult to demount the devices from a building after an earthquake since they are heavy with a weight of tens of *kN*.

In response to the engineering needs in practice for field inspection of the BRB, in 2014 Tsai and Wang [21] first presented an experimental study on an all-steel buckling restrained brace with windowed lateral support elements. The windows were opened only on the lateral support elements to allow inspection of the steel core without demounting or dismantling the BRB device. In this study, an all-steel BRB with inspection windows opened on the buckling-restraining unit was proposed. The scaled all-steel BRBs were tested under cyclic loadings. The investigation demonstrates that the inspection windows opened on the proposed BRB have insignificant influence on the strength of the device. The proposed device meets the design requirements and is thus considered as a damping apparatus with stable energy dissipation characteristic.

2. All-Steel Buckling Restrained Brace with Inspection Windows

The proposed all-steel MC-BRB consists of a single flat steel core and a buckling-restrained unit that includes constraining and lateral support elements with inspection windows, as shown in Fig. 2. Fig. 3 shows various



types of designs of the steel core and Fig. 4 gives two types of designs for the lateral support elements. All of the steel core plates used in this study have a multi-curved shape through an enlarged segment in the middle length of the MC-BRB to construct two energy dissipation segments. Figs. 5 and 6 demonstrate the sizes and locations of inspection windows opened on the weak and strong axes of the constraining elements, respectively.

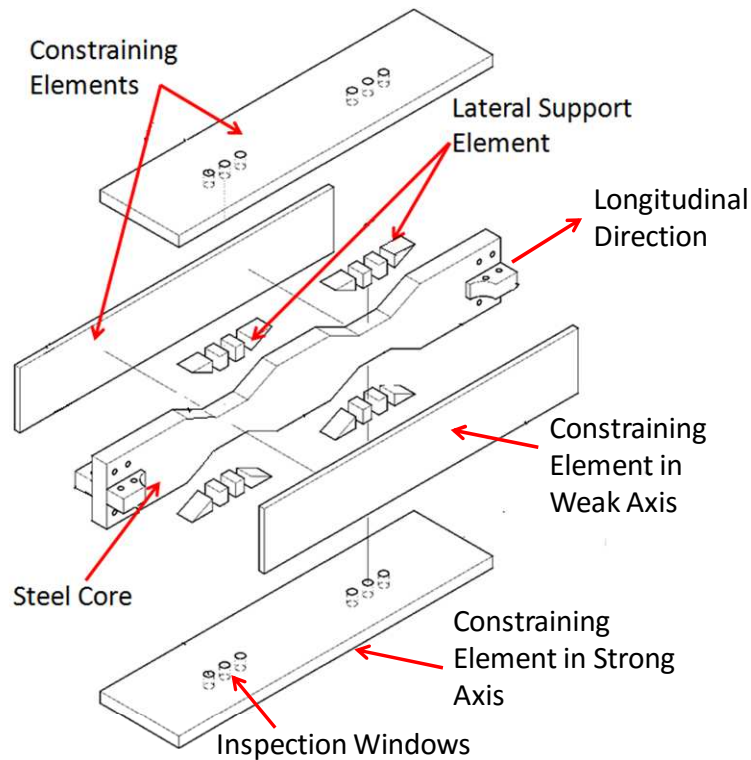


Fig. 2 – An exploded perspective view of proposed all-steel MC-BRB with inspection windows

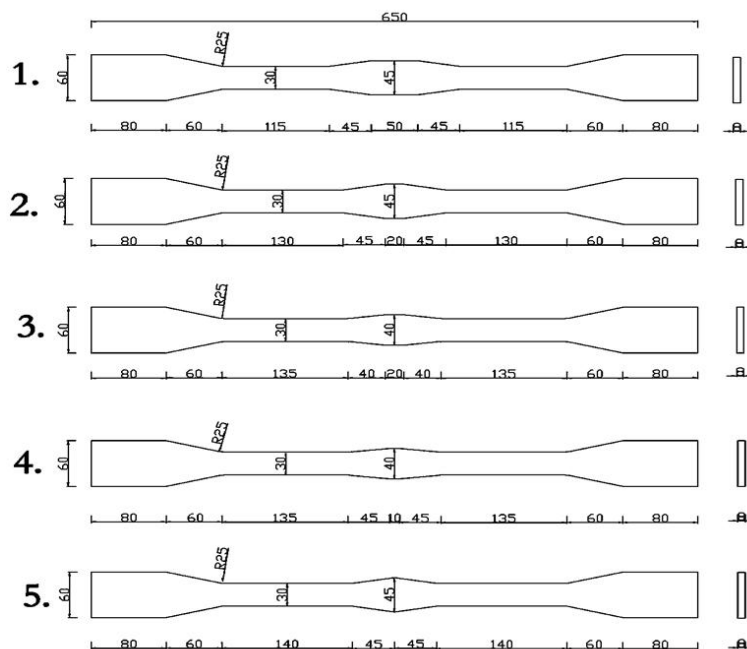


Fig. 3 – Types of steel core (unit: mm)

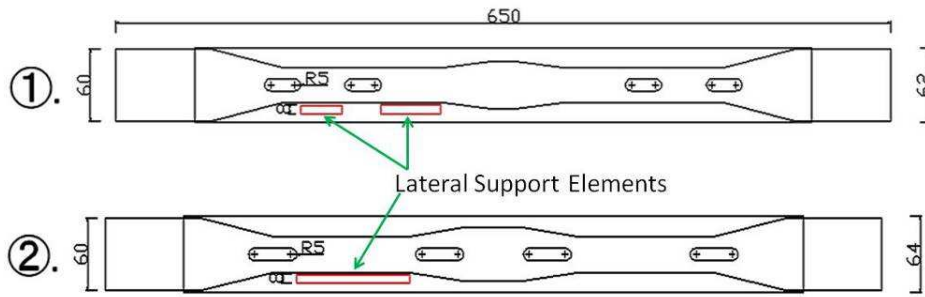


Fig. 4 – Types of lateral support elements (unit: mm)

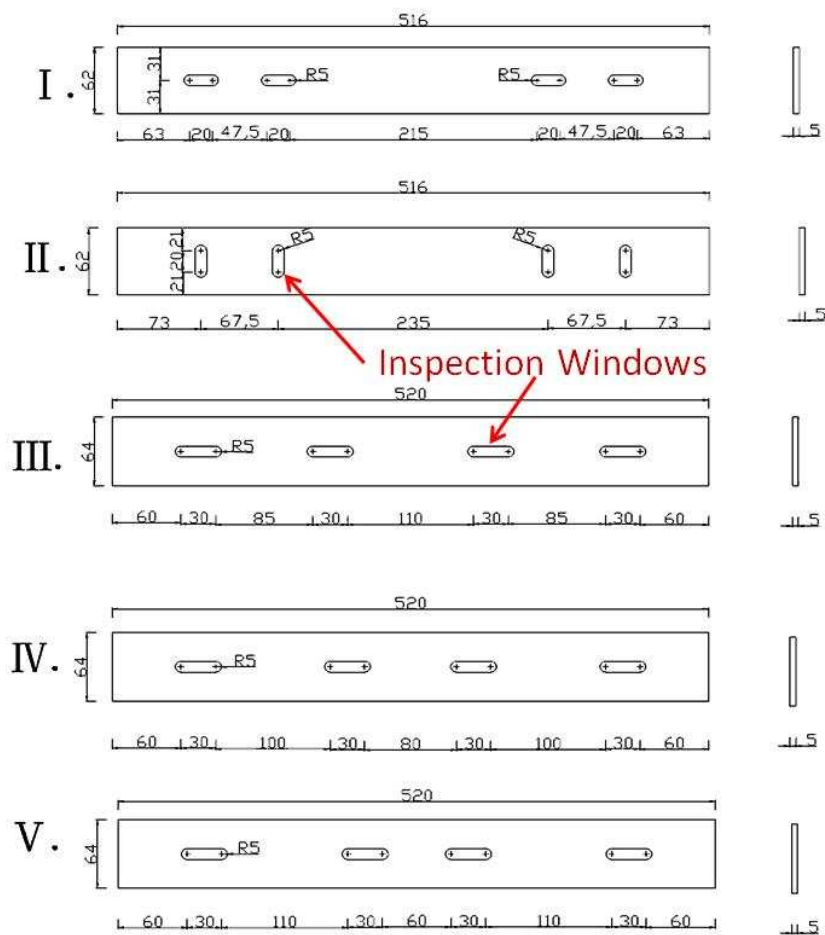


Fig. 5 – Types of inspection windows in weak axis of constraining elements (unit: mm)

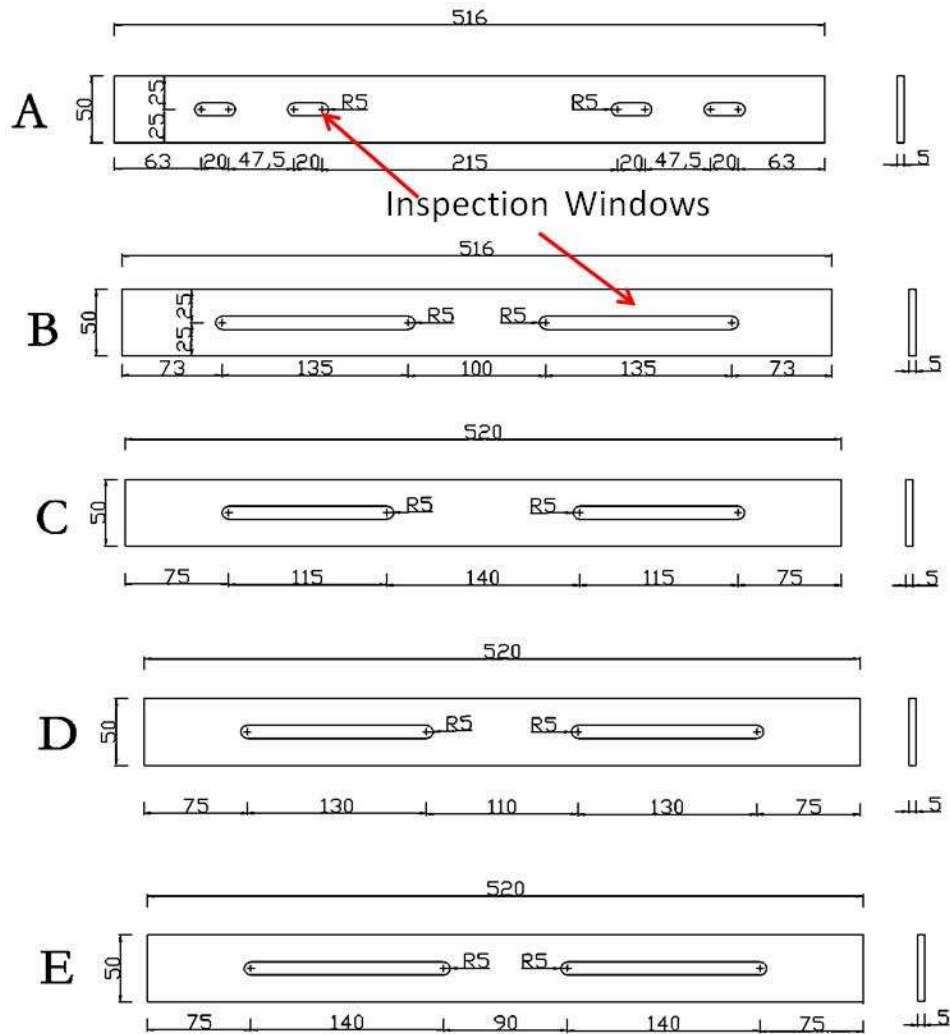


Fig. 6 – Types of inspection windows in strong axis of constraining elements (unit: mm)

Table 1 characterizes the types of BRB specimens, steel cores and inspection windows designed for this investigation. Seven all-steel MC-BRBs with various types of steel cores and inspection windows were reported in this paper. Specimens 7, 8, 13 and 14 have no lateral support element. Specimens 4 and 8 have inspection windows in the transverse direction that is vertical to the longitudinal direction in the weak axis. Other specimens have inspection windows in the longitudinal direction in the weak axis. As shown in Fig. 5, there are two inspection windows on the constraining element corresponding to each energy dissipation segment in the weak axis. All inspection windows in the strong axis are in the longitudinal direction, as shown in Fig. 6. The specified minimum yield stress of the steel core plates of the MC-BRB is 250 MPa . The energy dissipation segment is 30 mm in width and 8 mm in thickness, which results in a nominal yield force of 60.0 kN . The length of the energy dissipation segment was varied in order to examine the stress concentration around the regions close to the intersection of the energy dissipation segment and the enlarged segment. Note that the enlarged segments were welded to the constraining elements to have higher buckling strength and the connection between the lateral support elements and the constraining elements were also welded.



Table 1 – Types of specimens of MC-BRB

Specimen No.	Types of steel core	Types of Lateral Support	Types of Windows in Weak Axis	Types of Windows in Strong Axis
4	3	1	II	A
7	4	No	I	B
8	4	No	II	B
9	2	2	IV	D
10	5	2	V	E
13	1	No	III	C
14	2	No	IV	D

The stiffness of an MC-BRB with a steel core shown in Fig. 7, K_b , is given by [15, 20, 21]

$$K_b = \frac{k_1 k_2 k_3 k_4 k_5}{S} \quad (1)$$

where

$$S = 2k_2 k_3 k_4 k_5 + 2k_1 k_3 k_4 k_5 + 2k_1 k_2 k_4 k_5 + 2k_1 k_2 k_3 k_5 + k_1 k_2 k_3 k_4 \quad (2)$$

and where

$$k_1 = \frac{EA_1}{L_1} \quad (3)$$

$$k_2 = \frac{E(A_2 - A_1)}{L_2(\ln A_2 - \ln A_1)} \quad (4)$$

$$k_3 = \frac{EA_3}{L_3} \quad (5)$$

$$k_4 = \frac{E(A_3 - A_1)}{L_4(\ln A_3 - \ln A_1)} \quad (6)$$

and

$$k_5 = \frac{EA_5}{L_5} \quad (7)$$

Also, E , A_i and L_i are the elastic modulus, cross sectional area and length of the i^{th} segment, respectively.

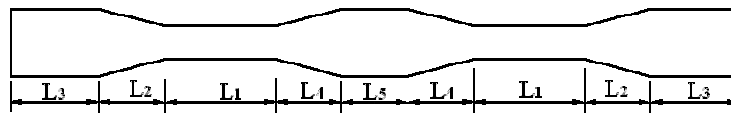


Fig. 7 – Steel core of MC-BRB

3. Experimental Results and Discussion

With reference to the Recommended Provisions for Buckling-Restrained Braces (AISC 2010) [22], the design of the braces should base upon results from qualifying cyclic tests in accordance with the procedures and acceptance criteria suggested in the Provisions' Appendix. As a rigorous testing, the following loading sequence including the standard and low-cycle fatigue loading protocols should be applied to the test specimen, where the deformation is the axial deformation of the core plate:



1. 2 cycles of loading at the deformation corresponding to $\Delta_b = \Delta_{by}$
2. 2 cycles of loading at the deformation corresponding to $\Delta_b = 0.5\Delta_{bm}$
3. 2 cycles of loading at the deformation corresponding to $\Delta_b = 1.0\Delta_{bm}$
4. 2 cycles of loading at the deformation corresponding to $\Delta_b = 1.5\Delta_{bm}$
5. 2 cycles of loading at the deformation corresponding to $\Delta_b = 2.0\Delta_{bm}$
6. Additional complete cycles of loading at the deformation corresponding to $\Delta_b = 1.5\Delta_{bm}$ as required for the Brace

Test Specimen to achieve a cumulative inelastic axial deformation of at least 200 times the yield deformation. Δ_b is the deformation quantity used to control loading of test specimens, Δ_{by} denotes the axial deformation at the first significant yield of the specimen, and Δ_{bm} that was assumed to be equal to $4.0\Delta_{by}$ depicts the axial deformation of the specimen at the design story drift.

The component tests of the scaled all-steel MC-BRBs specimens under cyclic loadings using an MTS test machine with a capacity of 250 kN were carried out in the Department of Civil Engineering at Feng Chia University, Taichung, Taiwan. The load-deformation responses of the standard tests with a maximum strain, ϵ_{max} , of 3.3% of the specimens are shown in Figs. 8 and 9, and the results for low-cycle fatigue tests with a strain of 2.5% are shown in Figs. 10 and 11. It should be noted that the negative values of the loads and deformations shown in these figures represent that the specimens were subjected to compressive loadings, and were otherwise subjected to the tensile loadings. There existed a flat in the early several nonlinear cycles because the strains in these cycles were still within the plateau area of the stress-strain curve of the material. Table 2 lists the comparison between the measured and theoretical elastic stiffness calculated by Eq. (1) and yield displacements. The nominal yield force of the steel core P_{yn} is 60 kN and the material overstrength factor R_y in Table 2 is 1.11 which was obtained from the coupon test. The theoretical results of the stiffness and yield displacement are in good agreement with the measured data. Table 3 lists the test results of the compression strength adjustment factor, β , which represents the ratio of the maximum compressive force to the maximum tensile force under the same displacements during the standard test, and the cumulative inelastic axial deformation capacity, η , representing the ratio of the accumulated inelastic deformation until failure of the tested specimen to the first significant yield deformation under the low cycle test. The compression strength adjustment factor for all tested specimens shown in this table is much smaller than the value (<1.30) required by the 2010 AISC Provisions. Experimental results listed in this table indicate that the proposed BRB with inspection windows satisfies all the requirements of the 2010 AISC Provisions and that the measured cumulative inelastic axial deformation capacity, η , is close to the theoretical value of $1.136 = (1+2\epsilon_{max})^2$ which was derived by Tsai et al. [20]. In addition, hysteresis loops presented in Figs. 10 and 11 give the results of the low-cycle fatigue test of the tested specimens. The test results of the cumulative inelastic axial deformation capacity listed in Table 3 are much higher than the value of at least 200 required by the 2010 AISC Provisions.

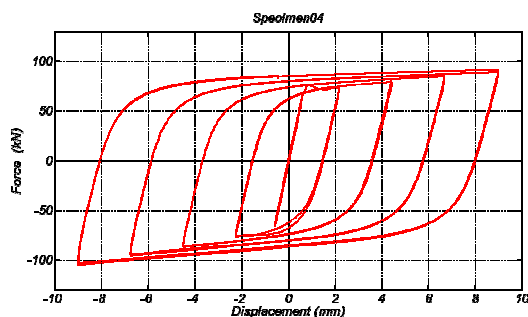


Fig. 8 – Hysteretic loops of the standard test of specimen 4 of all-steel MC-BRB

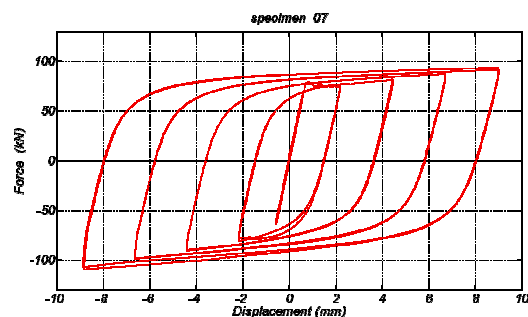


Fig. 9 – Hysteretic loops of the standard test of specimen 7 of all-steel MC-BRB

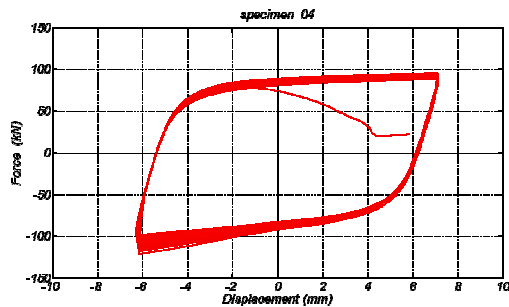


Fig. 10 – Hysteretic loops of the low cycle fatigue test of specimen 4 of all-steel MC-BRB

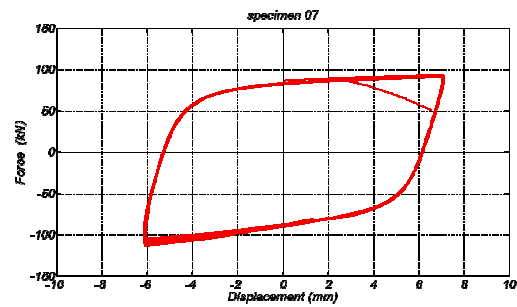


Fig. 11 – Hysteretic loops of the low cycle fatigue test of specimen 7 of all-steel MC-BRB

Table 2 – Comparison of experimental and theoretical results

Specimen No.	$K_{b(\text{exp})}$ (kN/mm)	$K_{b(\text{theory})}$ (kN/mm)	P_{ya} (kN)	$\Delta_{by} = \frac{R_y P_{yn}}{K_{theory}}$ (mm)	$\Delta_{by} = \frac{P_{ya}}{K_{exp}}$ (mm)
04	109.2	105.5	76.1	0.631	0.697
07	111.6	103.8	79.7	0.642	0.714
08	106.2	103.8	77.8	0.642	0.732
09	118.3	106.9	68.9	0.623	0.582
10	113.2	104.9	69.6	0.635	0.615
13	108.9	113.4	68.4	0.587	0.629
14	118.2	106.9	66.3	0.623	0.561

Table 3 – Test results of MC-BRB with various types of inspection windows

Specimen No.	Directions of Windows	T_{max} (kN)	P_{max} (kN)	β	η (Δ_{by})
4	Transverse	91.43	105.0	1.148	1151
7	Longitudinal	93.49	109.1	1.167	1021
8	Transverse	91.20	102.0	1.118	763*
9	Longitudinal	82.77	98.37	1.188	1387
10	Longitudinal	82.07	87.02	1.060	1336
13	Longitudinal	81.11	90.53	1.116	1271
14	Longitudinal	83.05	89.86	1.082	1703

*Testing stopped since the test machine was overheated.

As indicated in Figs. 12-15, the inside condition of the steel core can be monitored through inspection windows opened on the constraining elements during and after testing. Necking and rupture under tensile force and occasionally accompanied local buckling occurred in one of the energy dissipation segments of the steel core at the last cycle of fatigue testing. Figs. 16 and 17 respectively show the open-up view of Specimens 4 and 7 after testing. These two pictures verify the observations through the inspection windows, which were demonstrated in Figs. 12 and 13 for Specimen 4 and Figs. 14 and 15 for Specimen 7. The constraining elements with inspection windows provided good support to the steel core without yielding, and there was no sign of global buckling at the steel core plates, constraining elements or lateral support elements. These test results show excellent stable hysteretic behavior and satisfactory inelastic axial deformation capacity. Based on the experimental observations, the inspection windows on the strong and weak axes of the constraining elements had no significant effects on the strength and behavior of the proposed all-steel MC-BRB, and provided an easy and excellent function to enable engineers to inspect the inner steel core plate in the field after cyclic loadings without demounting or dismantling the devices.



Fig. 12 – Observation from inspection windows on weak axis (specimen 4)

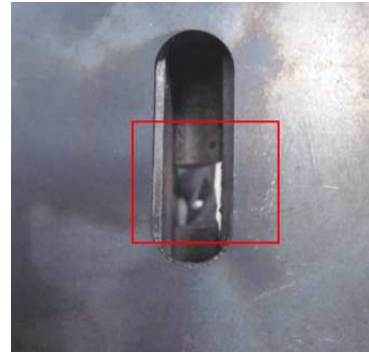


Fig. 13 – Observation from inspection windows on strong axis (specimen 4)



Fig. 14 – Observation from inspection windows on weak axis (specimen 7)



Fig. 15 – Observation from inspection windows on strong axis (specimen 7)

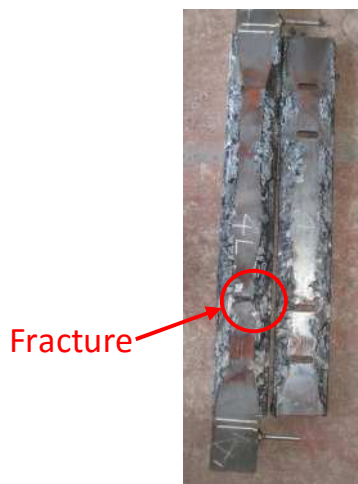


Fig. 16 – Open-up view of specimen 4

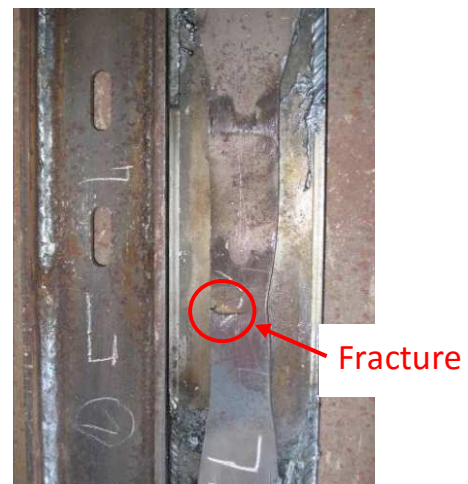


Fig. 17 – Open-up view of specimen 7



4. Conclusion

Various types of scaled all-steel multi-curve buckling-restrained braces (MC-BRBs) with inspection windows were investigated experimentally. On the basis of the experimental results and observations, no sign of global buckling or strength deterioration was observed, and the buckling-restrained unit with inspection windows still provided good support to the steel core without any damage. Welding the enlarged segment located in the middle of the steel core to the buckling-restrained unit could enhance the elastic stiffness of an all-steel MC-BRB, stabilize the whole device, prevent the sliding of the buckling-restraining unit and lead to smaller yield deformation. The conditions and damage levels of the steel core can be clearly observed through the inspection windows without demounting the device from a building or dismantling the device. The mechanical behavior of the BRB with inspection windows on constraining elements is stable and the fracture of the BRB always occurs at the energy dissipation segments after low-cycle fatigue tests. The difference between the maximum tensile and maximum compressive forces is small, and the cumulative inelastic deformation capacity is far better than the requirement of the test protocols. The test results show that the proposed BRB with inspection windows is thus considered as a stable energy dissipation apparatus.

5. References

- [1] Hollander M B (1966): Prestressed tubes and rods. US Patent No. 3232638.
- [2] Wakabayashi M, Nakamura T, Kashibara A, Morizono T, Yokoyama H (1973): Experimental study of elasto-plastic properties of precast concrete wall panels with built-in insulating braces. *Summaries of Technical Papers of Annual Meeting, Architectural Institute of Japan, Structural Engineering Section 10*, 1041-1044, in Japanese.
- [3] Kimura K, Yoshizaki K, Takeda T (1976): Tests on braces encased by mortar in-filled steel tubes. *Summaries of Technical Papers of Annual Meeting, Architectural Institute of Japan*, 1041-1042, in Japanese.
- [4] Mochizuki S, Murata Y, Andou N, Takahashi S (1979): Experimental study on buckling of unbounded braces under axial forces: Parts 1 And 2. *Summaries of Technical Papers of Annual Meeting, Architectural Institute of Japan*, 1623–1626, in Japanese.
- [5] Wada A, Connor J, Kawai H, Iwata M, Watanabe A (1992): Damage tolerant structures. *Proceeding 5th U.S.-Japan Workshop on the Improvement of Structural Design and Construction Practices, Applied Technology Council, ATC-15-4*, 27-39, San Diego, CA.
- [6] Black CJ, Makris N, Aiken ID (2002): Component testing, stability analysis and characterization of buckling-restrained braces. *Journal of Structural Engineering, ASCE*, **130**(6), 880-894.
- [7] Merritt S, Uang CM, Benzoni G (2003): Subassemblage testing of Corebrace buckling-restrained braces. *Report No. TR-2003/01, Structural Systems Project, Department of Structural Engineering, UC San Diego*.
- [8] Merritt S, Uang CM, Benzoni G (2003): Uniaxial testing of associated bracing buckling-restrained braces. *Report No. TR-2003/05, Structural Systems Project, Department of Structural Engineering, UC San Diego*.
- [9] Di Sarno L, Manfredi G (2010): Seismic retrofitting with buckling restrained braces: Application to an existing non-ductile RC framed building. *Soil Dynamics and Earthquake Engineering*, **30**(11), 1279-1297.
- [10] Di Sarno L, Manfredi G (2012): Experimental tests on full-scale RC unretrofitted frame and retrofitted with buckling restrained braces. *Earthquake Engineering and Structural Dynamics*, **41**(2), 315-333.
- [11] Chen CC (2000) Seismic behavior and design of buckling inhibited braces and ductile CBF's. *Structural Engineering*, **15**(1), 53-78, in Chinese.
- [12] Tsai CS, Chiang TC, Chen BJ, Chen WS, Yu SH (2004): Component test and mathematical modeling of advanced unbonded brace. *The 2004 ASME PVP Conference, Seismic Engineering*, V. C. Matzen and S. Fujita, editors, San Diego, California, U. S. A, PVP2004-2958, (486)2, 231-236.
- [13] Tsai CS, Chen WS, Chen KC (2005): Shaking table test of structure with reinforced buckling restrained braces. *the 2005 ASME PVP Conference, Seismic Engineering*, C. S. Tsai, editor, Denver, Colorado, U.S.A., **8**, 307-312.



- [14] Tsai CS, Chen WS, Chen BJ (2006): Component tests and simulation of advanced buckling restrained braces. *the ASME 2006 Pressure Vessels and Piping Conference, Seismic Engineering*, Vancouver, Canada, PVP2006-ICPVT11-93491.
- [15] Tsai CS, Chen WS, Lin YC (2008): Full scale shaking table tests of a steel structure with multi-Curve buckling restrained braces. *the 14th World Conference on Earthquake Engineering*, Paper No. 05-06-0007, Beijing, China.
- [16] Tsai CS, Lin YC, Chen WS, Su HC (2009): Mathematical modeling and full-scale shaking table tests for multi-curve buckling restrained braces. *Earthquake Engineering and Engineering Vibration*, **8**(3), 359-371.
- [17] Ma N, Wu B, Zhao J, Li H, Ou J, Yang W (2008): Full scale test of all-steel buckling restrained braces. *the 14th World Conference on Earthquake Engineering*, Beijing, China, Paper No. 11-0208.
- [18] Eryasar M, Topkara C (2010): An experimental study on steel-encased buckling-restrained brace hysteretic dampers. *Earthquake Engineering and Structural Dynamics*, **39**, 561-581.
- [19] Zhao J, Wu B, Ou J (2011): A novel type of angle steel buckling-restrained brace: Cyclic behavior and failure mechanism. *Earthquake Engineering and Structural Dynamics*, **40**, 1083-1102.
- [20] Tsai CS, Su HC, Chiang TC (2012) Huge scale tests of all-steel multi-curve buckling restrained braces. *the 15th World Conference on Earthquake Engineering*, Lisbon, PORTUGAL.
- [21] Tsai CS, Wang YM (2014): Experimental study of all-steel buckling restrained brace with windowed lateral support elements. *the 2014 ASME Pressure Vessels and Piping Conference, Seismic Engineering*, Anaheim, California, USA, PVP2014-28250.
- [22] AISC (2010): Seismic provisions for structural steel buildings. Appendix Part I, AISC.

6. Nomenclature

Δ_b	Deformation quantity used to control loading of test specimen (<i>mm</i>)
Δ_{bm}	Value of deformation quantity, Δ_b , corresponding to the design story drift. (<i>mm</i>)
Δ_{by}	Value of deformation quantity, Δ_b , at first significant yield of test specimen. (<i>mm</i>)
P_{ya}	Actual yield force of the steel core of an MC-BRB (<i>kN</i>)
P_{yn}	Nominal yield force of the steel core
K_b	Elastic stiffness of an MC-BRB (<i>kN / mm</i>)
$\Delta_{b,max}$	Measured maximum deformation of the steel core plate of an MC-BRB (<i>mm</i>)
ε_{max}	Tested maximum strain in the regions of energy dissipation segments of the specimen (%)
P_{max}	Measured maximum compressive force (<i>kN</i>)
T_{max}	Measured maximum tensile force (<i>kN</i>)
β	Compression strength adjustment factor
ω	Tension strength adjustment factor
η	Cumulative inelastic deformation capacity (Δ_{by})
F_y	Nominal yield force of the steel core
R_y	Material overstrength factor